Global shape processing: Which parts form the whole?

Jason Bell McGill Vision Research, Department of Ophthalmology, McGill University, Montreal, Quebec, Canada

Sarah Hancock School of Psychology, University of Nottingham, Nottingham, UK

Frederick A. A. Kingdom McGill Vision Research, Department of Ophthalmology, McGill University, Montreal, Quebec, Canada

Jonathan W. Peirce School of Psychology, University of Nottingham, Nottingham, UK

Research suggests that detection of low-frequency radial frequency (RF) patterns involves global shape processing and that points of maximum curvature (corners) contribute more than points of minimum curvature (sides). However, this has only been tested with stimuli presented at the threshold of discriminability from a circle. We used RF pattern adaptation to (a) examine whether a supra-threshold RF pattern is processed as a global shape and (b) determine what the critical features are for representing its shape. We measured the perceived amplitude shift of an RF test pattern after prolonged exposure either to a higher amplitude pattern or to various combinations of its parts (*concave* maxima, *convex* maxima, inflections). We found greater shifts in perceived amplitude after adaptation to a "whole" pattern than after adaptation to its component parts, which alternated to produce equal net contrast. Furthermore, when adapting to specific parts of the shape in isolation, we found that each part generated a similar magnitude aftereffect. Although the whole is clearly greater than the sum of the parts, we find that *concave* maxima, *convex* maxima, and inflections contribute equally to global shape processing, a fact that is only apparent when using a supra-threshold appearance-based task.

Keywords: shape, global, local, adaptation, aftereffects

Citation: Bell, J., Hancock, S., Kingdom, F. A. A., & Peirce, J. W. (2010). Global shape processing: Which parts form the whole?. *Journal of Vision, 10*(6):16, 1–13, http://www.journalofvision.org/content/10/6/16, doi:10.1167/10.6.16.

Introduction

The recognition of visual objects involves multiple stages of processing. Cortical area V1 contains neurons that detect oriented lines and edges (Hubel & Wiesel, 1968; Kapadia, Westheimer, & Gilbert, 2000). Areas such as V4 contain neurons responsive to more complex patterns such as curved contours (Muller, Wilke, & Leopold, 2009; Pasupathy & Connor, 1999, 2001, 2002) and concentric patterns (Dumoulin & Hess, 2007; Gallant, Braun, & Van Essen, 1993; Gallant, Connor, Rakshit, Lewis, & Van Essen, 1996; Wilkinson et al., 2000) and higher areas such as IT and LOC appear to contain neurons specialized for the detection and recognition of whole objects (Grill-Spector, Kushnir, Edelman, Itzchak, & Malach, 1998; Hayworth & Biederman, 2006; Kourtzi & Kanwisher, 2001; Wilkinson et al., 2000). However, while it is widely accepted that the human visual system contains neurons selective for both the component features of objects as well the objects themselves, our understanding of which types of local features are combined into whole objects is far from complete. The present communication examines the relative contributions of different types of local features to the global representation of closed-contour shapes.

The outline contour of an object is a sufficient cue for its recognition (Attneave, 1954; Biederman, 1987). In particular, Attneave suggests that points along outline contours that deviate from a straight line, such as corners, are the most important for object recognition, a principle successfully utilized in "dot-to-dot" drawings. A popular stimulus among vision scientists used to study the relative importance of different local features in global shape processing is the Radial Frequency, or RF pattern (Bell, Badcock, Wilson, & Wilkinson, 2007; Hess, Wang, & Dakin, 1999; Loffler, Wilson, & Wilkinson, 2003; Wilkinson, Wilson, & Habak, 1998). The RF pattern is a perturbed circle that can be characterized by its average radius, amplitude, and radial frequency (see Figure 1). RF patterns can be used to represent simple closed-contour shapes like triangles and squares. By combining RFs of different radial frequency, complex patterns such as fruit shapes and human body parts can be created (Wilkinson, Shahjahan, & Wilson, 2007; Wilson & Wilkinson, 2002; Wilson, Wilkinson, Lin, & Castillo, 2000). One of the main advantages of RF patterns over line drawings of objects is that they afford

doi: 10.1167/10.6.16 Received September 24, 2009; published June 17, 2010 ISSN 1534-7362

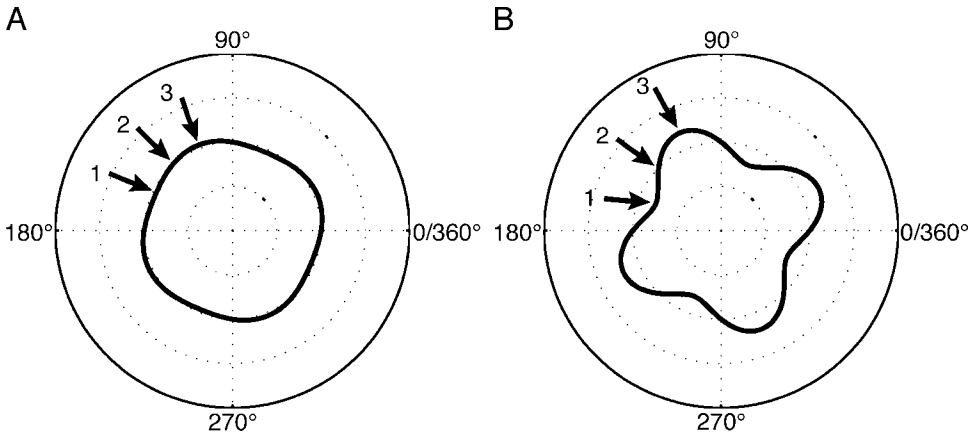

Figure 1. An illustration of two different amplitude RF4 patterns, including the location of particular features along the boundary. (A) At low pattern amplitude (near threshold). (1) The trough of the modulation function, also referred to as the point of minimum curvature, or "side", (2) the zero crossing, (3) the peak of the modulation function, also called the point of maximum curvature, *convex*. (B) At higher amplitude (well above detection threshold). (1) The trough of the modulation function, now a point of maximum *concave* curvature, (2) the zero crossing now corresponds to an inflection (although the two are not always at the same point on the contour), (3) the peak of the modulation function, still a point of maximum *convex* curvature.

parametric control of local feature content. In the current study, we sought to answer two main questions about the processing of these patterns: (1) is the percept of the whole greater than the sum of its parts and (2) do all parts of the pattern contribute equally to the global percept?

RF shape studies have consistently reported that for relatively low-frequency RF patterns (<RF10), information from all cycles is used to discriminate the pattern from a circle; in other words, there is global pooling of form information (Bell & Badcock, 2008, 2009; Hess, Achtman, & Wang, 2001; Hess et al., 1999; Jeffrey, Wang, & Birch, 2002; Loffler et al., 2003; Wilkinson et al., 1998). These studies all measured the ability to discriminate RF shapes from circles, i.e., they used near-threshold amplitude patterns. However, to accurately represent simple (e.g., triangle) or complex (e.g., pieces of fruit) shapes, RF patterns need to have higher amplitudes (Poirier & Wilson, 2006; Wilson & Wilkinson, 2002), so it would seem sensible to use these. In the first part of the study, we investigate whether a supra-threshold RF pattern is processed as a global form or just as its parts.

Near-threshold studies of RF processing have also examined which parts of the contour are spatially integrated by the global shape mechanism. While the evidence suggests that all cycles are used to discriminate the pattern from a circle (Bell & Badcock, 2008; Hess et al., 1999; Loffler et al., 2003), this does not mean that all of the form information present *within* each cycle is used. Several researchers have reported that the points of maximum convex curvature, i.e., the "corners" in an RF pattern, are the most important features for detecting the pattern's global shape, with the zero crossings second in line of importance, and the points of minimum curvature, i.e., the "sides," least important (Bell, Dickinson, & Badcock, 2008; Habak, Wilkinson, Zakher, & Wilson, 2004; Loffler et al., 2003; Poirier & Wilson, 2007). Others, however, have argued for a more significant role for "sides" (Hess et al., 1999; Kurki, Saarinen, & Hyvarinen, 2009; Mullen & Beaudot, 2002). Figure 1A (1–3) illustrates these features at near-threshold amplitude. Several studies have adopted the term "side" to describe the parts of the RF contour centered around the troughs of the waveform, analogous to the sides of a square (RF4) or pentagon (RF5; Hess et al., 1999; Loffler et al., 2003; Mullen & Beaudot, 2002). This analogy is somewhat misleading, however, because the "sides" on any given RF are only perceptually collinear at a single deformation amplitude, while at all other amplitudes they have either convex or concave curvature with respect to the shape's center. In this communication, we will use the terms "convex" and "concave" parts however to refer to the half-cycles of the contour centered, respectively, on the peaks and troughs of the RF pattern (with respect to the shape's center) rather than the terms "points of maximum" and "points of minimum" curvatures, which are ambiguous since they can refer either to a difference in the magnitude of curvature or a difference in its sign. We also use the term "inflection" to refer to the half-cycles of the contour centered around the zero crossings of the shape waveform, provided there is a change in the sign of curvature at the point. An inflection point is a finite point in space, so to study the contribution of inflections to shape processing we had to use stimuli that were extended either side of the inflection point.

The specific role of the concave parts of an RF shape has yet to be investigated. The reason for this, as Figure 1A demonstrates, is that at threshold amplitudes, low and

intermediate RFs possess neither concave parts nor inflections, making it difficult to assess their contribution. Figure 1B shows that at higher-than-threshold amplitudes the "sides" become concave curves and inflections begin to appear. Given that these features are only physically present at supra-threshold amplitudes, it is possible that the aforementioned order of importance of different local features might not hold for supra-threshold amplitudes. To test this hypothesis, we have examined the contributions of convexities, concavities, and inflections in the processing of the global shape of supra-threshold amplitude RF patterns.

In order to test global shape processing at supra-threshold amplitudes, we have switched from a performance-based to an appearance-based approach. We have utilized the fact that the perceived amplitude of an RF pattern can be altered by adaptation. Specifically, adaptation to an RF pattern causes a shift in the perceived amplitude of an RF pattern with slightly different amplitude in a direction away from that of the adapting stimulus, a phenomenon recently termed the radial frequency amplitude aftereffect, or RFAAE (Bell & Kingdom, 2009).

To determine the relative contribution of different parts of an RF pattern for global shape processing using the RFAAE as a tool, it is first necessary to establish whether a supra-threshold RF pattern is indeed processed as a "global" form, i.e., more than the sum of its parts. To this end, we have used the method of "compound adaptation," designed specifically to compare the effects of adaptation to the component parts with the effects of adaptation to the whole stimulus (Hancock & Peirce, 2008; Peirce & Taylor, 2006). The defining characteristic of this method is that the "whole adaptors" and "parts adaptors" are equated for exposure duration and intensity of components during adaptation. The rationale is that if the adaptive effect of the whole is greater than the parts, this indicates that an additional mechanism, sensitive to the whole rather than just the parts, has been adapted.

Our first experiment compares whole-RF and parts-of-RF adaptors on the size of the RFAAE in whole-RF test shapes. The second and third experiments then compare the size of the RFAAE in whole-RF test patterns for adaptors comprised of different RF parts, specifically convexities, concavities, or inflections, in order to determine their relative contributions to RF shape processing.

Methods

Participants

Two experienced psychophysical observers (authors, JB and SH) and three naive participants with normal or corrected-to-normal vision took part in the current study. The three naive observers took part on a voluntary basis.

Apparatus

The PsychoPy stimulus generation library (Peirce, 2007) was used to create and present the stimuli and to collect the data. Stimuli were presented on a computer-controlled cathode-ray-tube (CRT) monitor (Vision Master Pro 513, liyama) at a resolution of 1024 × 768 pixels and at a refresh rate of 85 Hz with a mean luminance of 49.56 cd/m^2. The monitor was driven by 14-bit digital-to-analogue converters (Bits++, Cambridge Research Systems, Cambridge, UK, http://www.crsltd.com). The monitor was calibrated using a photo-spectrometer (PR650, Photo Research, Chatsworth, CA, USA) to gamma-correct the red, green, and blue (RGB) guns independently and this gamma correction was verified psychophysically using a 2nd-order motion-nulling procedure (Ledgeway & Smith, 1994). The observer's head was stabilized in a chin rest 52 cm from the monitor with the viewable area subtending 43.6° of visual angle. Observers JB and LA collected data using the same PsychoPy stimulus generation library, but the stimuli were displayed on a Sony Trinitron G400 monitor, running at a resolution of 1024 × 768 and a refresh rate of 75 Hz with a mean luminance of 81 cd/m^2.

Stimuli

The stimuli were whole and part radial frequency (RF) patterns with a radial frequency of four cycles per 360°. Examples of whole shapes and part stimuli are shown in Figures 2B and 3B. The RF patterns were created in the same manner as described in previous studies (Wilkinson et al., 1998). The distance from the center of the pattern to the midpoint of the contour is specified by

$$r(\theta) = r_{\text{mean}}(1 + A\sin(\omega\theta + \varphi)), \quad (1)$$

where r and θ (expressed in degrees) specify the polar coordinates, r_{mean} is the average radius of the contour, A is the amplitude, ω is the radial frequency, and φ is the phase angle. The luminance profile through a radial cross-section of the contour was a fourth derivative of a Gaussian (D4; Wilkinson et al., 1998), with peak spatial frequency of 8 c/deg and sigma 3.0′. The contrast of the D4 pattern was set to 1.0. All RF patterns had a mean radius of 1.0°. The adapting patterns had amplitudes of 0.2°. The reference probe patterns had amplitudes of 0.1°.

The part stimuli were contours with a plateau at full contrast in the middle of the contour and two cosine-squared ramps that fell to a contrast of zero at the contour's ends. The ramps from the various parts were such that if they were added their contrast profiles would sum to 1. As a result, the sum of all the part stimuli (in terms of their luminance deviations from the gray background) was identical to the whole RF pattern. To generate the parts used in Experiment 1, the RF pattern was decomposed into

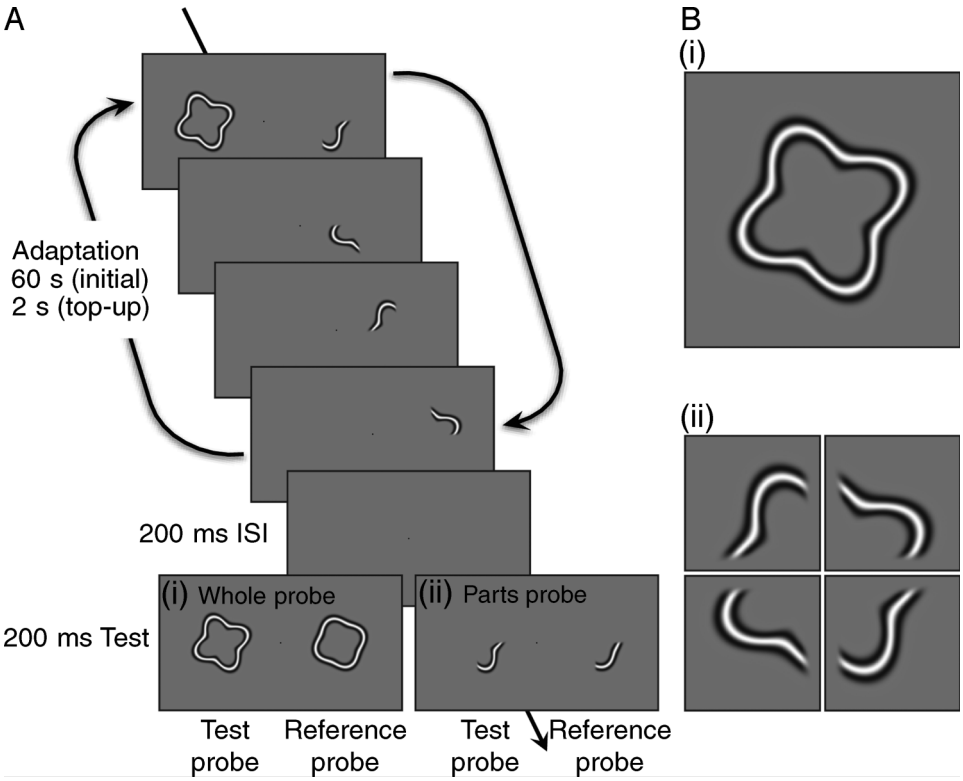

Figure 2. (A) Sample adaptation sequence: The illustration provides a schematic of the adaptation procedure for Experiment 1. Across each 2 s of adaptation, the observer was presented with the "whole" adaptor (500 ms) in one hemi-field and all four "parts" of the RF in 500-ms intervals. Following the 60 s of adaptation, the observer was presented with the probe stimuli, which were either (i) "whole" probes or (ii) "parts" probes. See Movie 1 for a demonstration. For this experiment, the reference probe amplitude was fixed at 0.1 deg and the test probe amplitude was varied according to a staircase procedure to find the PSE. On each trial, observers indicated which probe stimulus appeared to have the greater amplitude. Each observer performed a minimum of four staircases for each adapting configuration. (B) A large-scale illustration of the (i) "whole" and (ii) "parts" adapting stimuli.

four segments, each containing exactly one quarter of the pattern (one complete modulation cycle), in a continuous contour (see Figure 2Bii), which were presented individually. In Experiments 2 and 3, the parts stimuli each consisted of four 45° segments of contour (a half-modulation cycle). These segments were centered on (a) points of maximum concavity (Figure 3Bi, left), (b) points of maximum convexity (see Figure 3Bi, right), and (c) points of inflection in a clockwise or anti-clockwise direction (Figure 3Bii). The sum of the concave and convex part stimuli is identical to the whole pattern, as is the sum of the two inflection stimuli.

Procedure

Dual adaptor method RFAAE (Experiment 1): Participants were adapted to RF patterns in two patches of the visual field, centered 3.5° either side of the fovea on the horizontal meridian. The procedure is shown schematically in Figure 2A and also in Movie 1. In one visual hemi-field, the RF pattern was presented as a complete shape ("whole" field) and in the other the same pattern was decomposed into four parts, which were presented in alternation, each comprising one quarter of the stimulus. Exposure to each part of the RF pattern was equated in the two hemi-fields by presenting the "whole" shape for a quarter of the time (500 ms every 2 s), whereas the part stimuli alternated every 500 ms. The temporal phases of the alternations in each hemi-field were independently randomized so that no coherent motion was observed. The orientation of the overall stimulus was also randomized every 2 s (after each presentation of all four part stimuli) in order to reduce adaptation to local orientation. After the adaptation period, a probe stimulus was presented in each of the two adapted locations. The probes (shown in the bottom of Figure 2A) could either be a pair of full RF patterns ("whole" probe) or one pair of parts stimuli ("parts" probe), at a random orientation.

The initial period of adaptation lasted for 60 s and was "topped-up" with another 2 s of adaptation prior to each trial. This was followed by a 200-ms ISI, consisting of a mean gray screen, before presentation of the probe stimuli for 200 ms. A central fixation spot was visible for the entire trial. Observers pressed one of two keys to make a 2AFC response indicating the side on which the stimulus

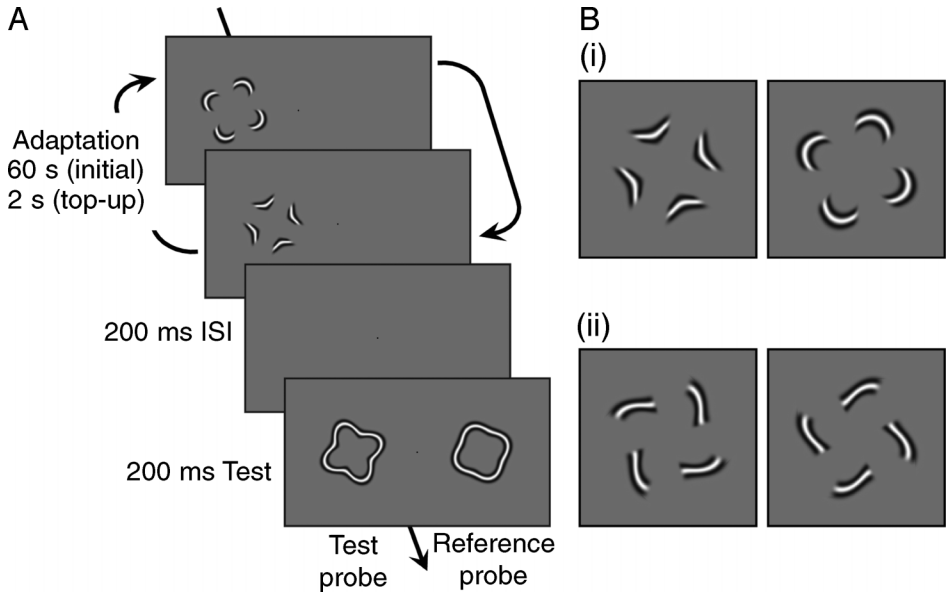

Figure 3. (A) A schematic of the adaptation sequence for Experiment 2 (single adaptor method). The adaptor was presented in one hemi-field only. Every 2 s, the observer was presented with two types of parts; alternating each second. Each part presented exactly one half of a complete RF pattern (see Methods section for a full description). Following adaptation, the observer was presented with two "whole" probes and was asked to indicate which appeared higher in amplitude. As before, the test probe was presented in the adapted field and the reference probe was presented in the unadapted field and fixed at an amplitude of 0.1. (B) Examples of the individual adapting patterns for Experiment 2: (i) concave and convex stimulus pair; (ii) inflection stimulus pair. For Experiment 3, these stimuli were presented in isolation during adaptation rather than in a pair and a blank gray screen was presented in the remaining 1 s of the adaptation sequence.

appeared to have greater amplitude. The response triggered the next trial to commence with another "top-up" adaptation period.

The reference probe (presented in the "parts" adaptor field) had a fixed amplitude. The amplitude of the test probe (presented in the "whole" adaptor field) was increased or decreased according to a one up one down staircase procedure based on the observers' responses, which was designed to hone in on the point at which the observer perceives the two probe stimuli to have the same amplitude (point of subjective equality (PSE)). The initial amplitude of the test probe was randomized to either 0.15 or 0.05 so observers could not predict the first response in any staircase. Step sizes started with an amplitude change of 0.02 and decreased after each reversal until they were 0.003, after which the step size was constant. Each probe type (whole shape and parts) was tested in separate staircases in different test sessions. Each staircase was terminated after 50 presentations of the probe stimuli (each run typically yielded around 30 reversals). To control for visual field biases, each observer collected a minimum of four staircases with the whole shape adaptor in the left hemi-field and four staircases with the whole shape adaptor in the right hemi-field for each probe type. Only one of these two configurations was tested in any one session and a minimum of 1 h was left between sessions to prevent crossover adaptation between conditions.

Single adaptor method RFAAE (Experiments 2 and 3): The procedure was the same as for Experiment 1 but now an adaptor was presented in only one visual hemi-field (see Figure 3A). In Experiment 2, the adaptor was one of (a) the whole RF pattern alternating with a blank field every 1 s, (b) a stimulus consisting of concavity and convexity stimuli alternating every 1 s (extrema, see Figure 3Bi), or (c) the two inflection stimuli alternating at the same rate (Figure 3Bii). The summed contrast of each pair of parts stimuli is equal to the whole RF pattern, so, as in Experiment 1, the overall exposure of the component segments was identical to that for the whole stimulus adaptor in all the adapting conditions. The probe stimuli were always whole RF shapes (as shown in Figure 3A).

In Experiment 3, the adaptor was a stimulus consisting of: concavity stimuli only (Figure 3Bi, left), convexity stimuli only (Figure 3Bi, right), or one half of all inflections (Figure 3Bii, left). In all cases, the adapting stimulus alternated with a blank field every 1 s. The part adaptor stimuli in Experiment 3 contain four half-cycle segments and therefore their summed contrast is equal to one half of the whole RF shape only.

Probe stimuli were whole RF patterns, presented in both hemi-fields so that the PSE could be determined in relation to an unadapted location. Each observer completed a minimum of four staircases with the adaptor in the left hemi-field and four staircases with the adaptor in the right hemi-field for each stimulus condition.

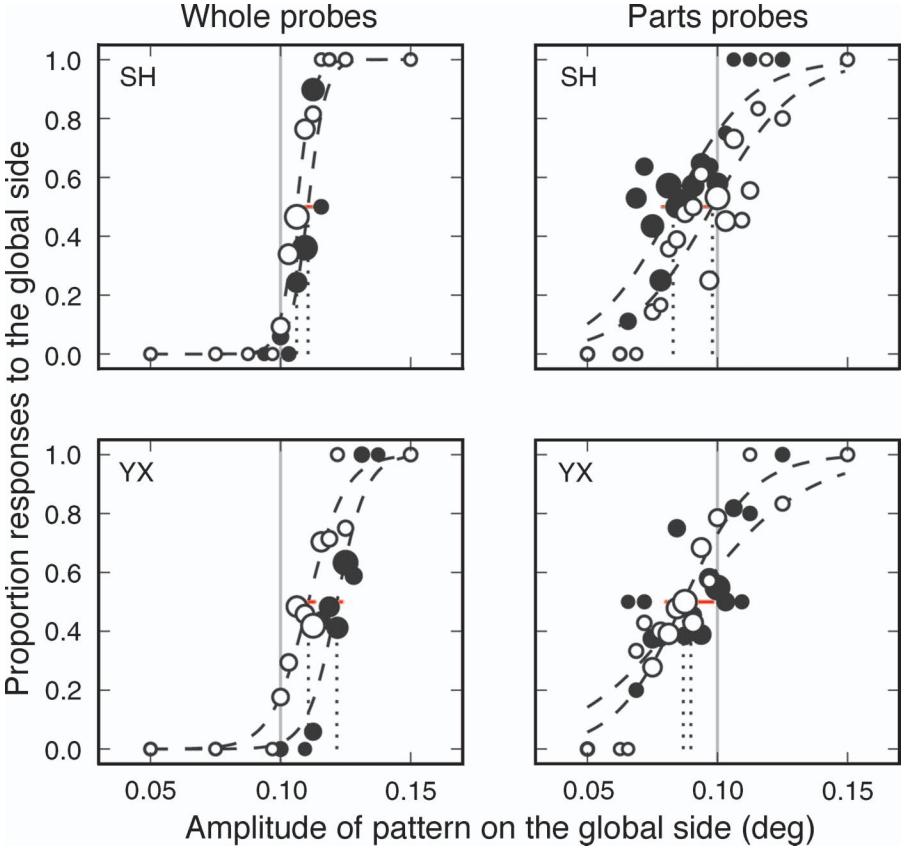

Figure 4. Sample psychometric functions for two observers (SH and YX), plotting the proportion of times that the test probe (corresponding to the "whole" or global adaptor hemi-field) was chosen as being higher in amplitude than the reference probe (corresponding to the "parts" adaptor hemi-field) for the (left) "whole" and (right) "parts" probe conditions. Dot sizes indicate the number of responses made at each amplitude (larger size = more responses; range = 1–88). The gray vertical line indicates the amplitude of the reference probe (fixed at 0.1). Unfilled and filled data points show data for conditions where the "whole" or global adaptor was to the left or right of fixation, respectively. Data were fit with a logistic function and bootstrapping was used to calculate error bars (95% CIs) around the PSE estimate. For both left and right conditions, the PSE (noted by dashed lines) in the "whole" probe conditions (left panels) is shifted horizontally to the right from the gray line, indicating that the test probe in the "whole" adapting field needed to be of greater physical amplitude than the reference probe ("parts" field) to appear equal in amplitude. This translates to there being greater adaptation to the "whole" adaptor than to the "parts" adaptor: when using "whole" test probes. This is not the case in the "parts" probe conditions (right panel).

Data analysis

We quantified the effect of adaptation as the amount of additional modulation amplitude required in the test probe for the test and reference probes to appear equal (the point of subjective equality, PSE) for each observer. For each condition and presentation side, the responses for each stimulus intensity level (test amplitude) that had been used in the staircases were averaged and a logistic function was fit to the resulting psychometric function. The PSE was derived from this fit as the point at which the observer was at 50% probability of reporting that the test probe had the greater amplitude. Using this method of binning, all data contribute to the calculation of the PSE, rather than only the trials on which reversals occur, and a full psychometric function can be recovered. It should be noted that data points near the PSE have more trials contributing to each point, as a result of the staircase procedure itself. The PSE values for each presentation side were averaged to account for any side bias in responding, producing a single PSE value derived from a total of at least 400 trials (50 $\times$ 4 on each side of presentation) for each condition.

To estimate the sampling error of the PSE values, a bootstrap procedure was used. For each condition, logistic functions were fit to 5000 within-subject bootstrap resamples from the 200 individual responses for each presentation side so that, for each resample, a whole new pair of psychometric functions could be derived (one for each presentation side). The PSE values for each pair of functions were averaged to account for side bias then used to derive 95% confidence intervals of the PSE for each

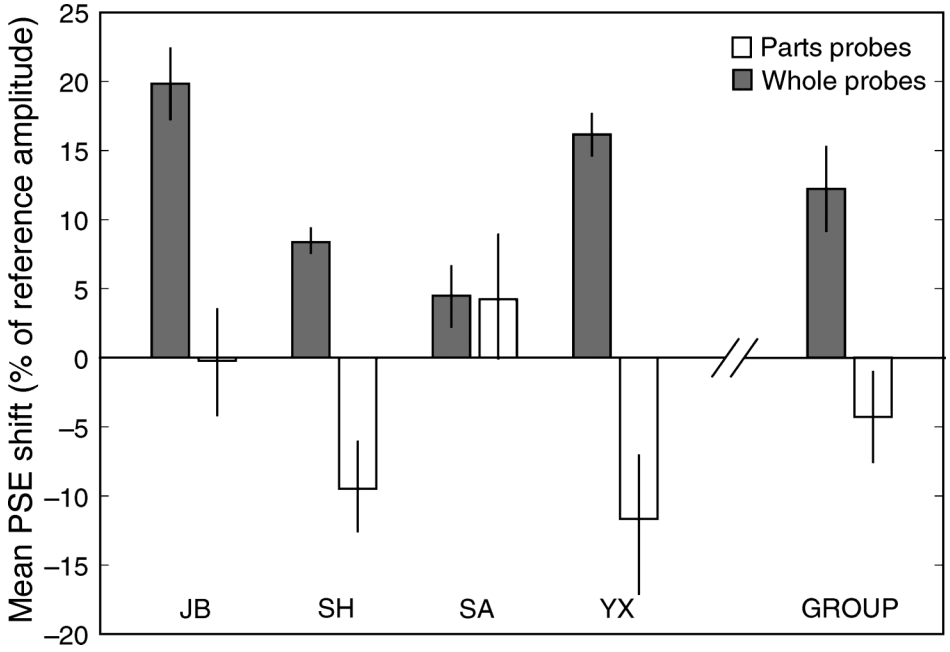

Figure 5. Magnitude of the global adaptation effect (mean PSE shift) given in terms of the percentage of the reference amplitude for whole shape (gray columns) and part probes (white columns) in Experiment 1 for individual observers and across the group. The black horizontal line represents the point of veridical equality as predicted by the null hypothesis. For the individual observer data, error bars represent 95% confidence intervals based on 5000 bootstrap resamples, and for the group average data, they represent ±1 *SEM* across observers (N = 4).

observer in each condition. Figure 4 shows sample data sets and psychometric functions with error bars for two observers in two different conditions.

Results

Experiment 1: Is the whole greater than the sum of the parts?

In Experiment 1, we directly compared the radial frequency amplitude aftereffect (RFAAE) induced by the whole shape with that induced by its parts presented in alternation. Observers adapted to a whole RF pattern in one visual field (the "whole" field) and the individual parts that comprised that pattern alternating in the other visual field (the "parts" field). The key aspect of this method is that the overall exposure to each part of the RF pattern is equal in both adapting locations/conditions. Therefore, if the RFAAE results simply from local orientation and/or curvature adaptation, then the size of the RFAAE in the two locations should be equal. If, however, the whole pattern is greater than the sum of its parts, then the aftereffect in the whole RF probe should be greater in the field corresponding to the whole adaptor than in the field corresponding to the parts adaptor. This would be indicated by a shift in the point at which the probe stimuli in the two adapted locations appeared to have equal amplitude (the PSE).

The average PSE shift measures the difference in adaptation effects between the two probe locations. This is shown for four observers in Figure 5, and for test probes comprising the whole RF pattern (gray bars) or a single part (white bars). The shift is given as a percentage of the reference amplitude. For whole pattern probes (gray bars), there is a greater effect of adaptation on the side of the whole adaptor (the 95% confidence intervals of the PSEs do not include zero). On average, the test probe pattern (in the whole-pattern-adapted field) required an extra 0.0123° ± 0.0035° of amplitude in order to be perceived as equal to the reference probe pattern, indicating a greater RFAAE on the whole-pattern-adapted side. Given that the reference amplitude was 0.1 deg, this is approximately a 12% greater shift in the perceived amplitude of the test probe relative to the reference probe. These results show that there was greater adaptation in the whole field than in the parts field, consistent with an aftereffect that is specific to the global form of the RF pattern.

With probe stimuli comprised of the parts of the pattern (Figure 5, white bars), no observer showed a significant positive shift in the PSE, consistent also with the previous result showing that the aftereffect in the whole pattern probe was specific to the global form of the stimulus. In the parts probe condition, the average PSE shift (±1 *SEM*) was −0.0043 ± 0.0038° (a −4.3% shift in the perceived

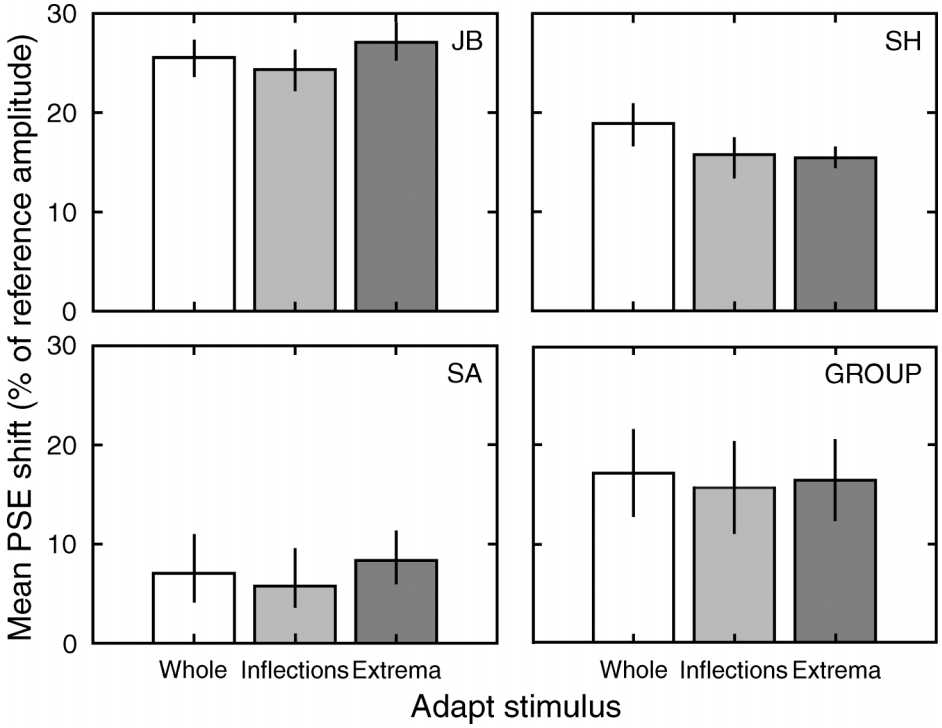

Figure 6. Magnitude of the adaptation effect (mean PSE shift) for a whole pattern, inflections, and extrema (convexities and concavities) adaptors in Experiment 2, for three observers. Zero on the *x*-axis represents the point of veridical equality as predicted by the null hypothesis. Error bars indicate 95% confidence intervals based on 5000 bootstrap resamples. Data are also shown averaged across observers. Error bars indicate ±1 *SEM* across observers (N = 3).

amplitude). This shows that on average the test probe required a 4.3% *smaller* amplitude than the reference probe for them to be perceived as equal, indicating a slightly greater adaptation in the parts hemi-field. This may reflect an effect of adaptation to local orientation and/or curvature but was only significantly different from zero for two of the four observers.

Figure 4 presents response data and fitted logistic functions for two observers (SH and YX). The data plot the proportion of times the test probe was chosen as being higher in amplitude than the reference probe for whole (left panels) and parts (right panels) probe conditions. Unfilled and filled circles show results for conditions where the whole adaptor was to the left or right of fixation, respectively. The vertical gray line indicates the amplitude of the reference probe. For the whole probe conditions (left panels), the PSE estimate (dashed lines) obtained from each fit is shifted horizontally to the right of this line, indicating that the whole test probe required significantly greater amplitude than the reference probe in order to be perceived as equal in amplitude. This is not the case for parts probe conditions (right panels), where the PSE estimate (dashed lines) obtained from each fit is now shifted horizontally to the left, indicating that the part test probe corresponding to the whole adaptor required less amplitude than the reference probe in order to be perceived as equal in amplitude.

The results of Experiment 1 clearly indicate that adaptation to the whole RF pattern is greater than that to its constituent parts, supporting the view that it is processed as a global form. However, this does not mean that all the information within the contour of the RF pattern is used. In the following experiments, we investigate the relative contributions of different parts of the pattern to the global shape representation.

Experiment 2: Comparing extrema with points of inflection

In Experiment 2, we aimed to examine whether the contour extrema (concavities and convexities) contribute more than the parts centered on the points of inflection to the RFAAE. Previous studies measuring thresholds for discriminating an RF from a circle have indicated that points of convexity (or "corners") are the most important features (Bell et al., 2008; Habak et al., 2004; Loffler et al., 2003). However, because the RF amplitudes used in these studies were close to threshold, there were no real concavities in the pattern (see Figure 1A). Here we use supra-threshold RF patterns to compare the relative adaptive strengths of curvature extrema with inflections and compare their adaptive strengths with that of a whole RF pattern. The procedure for Experiment 2 is shown schematically in Figure 3A and was described in full in the Methods section (Single adaptor method RFAAE). Examples of each adapting pair are shown in Figure 3B

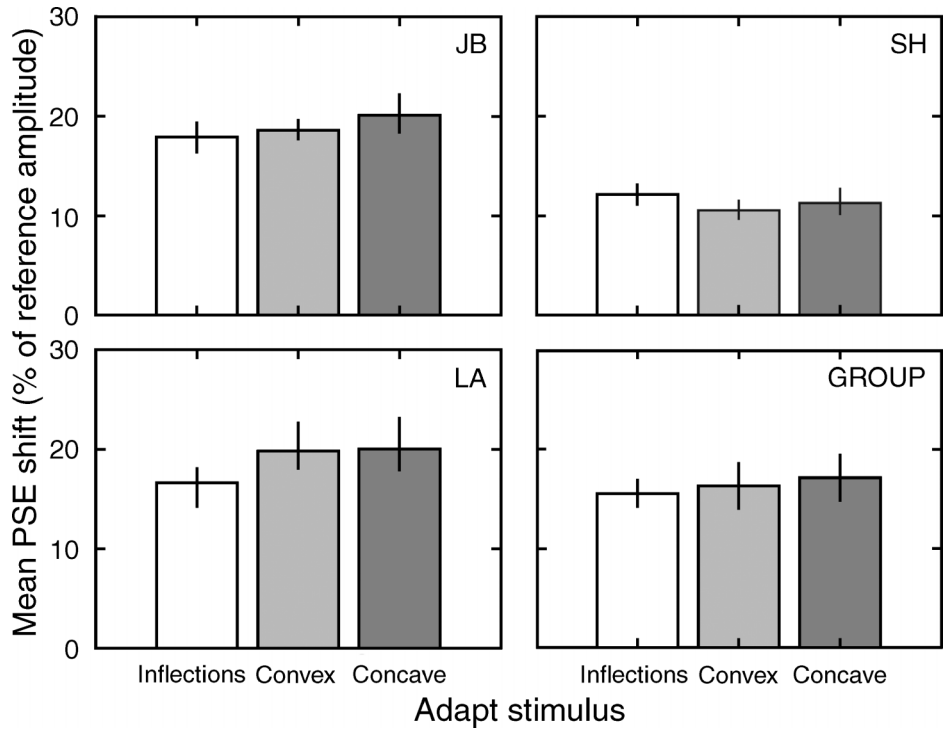

Figure 7. Magnitude of the adaptation effect (mean PSE shift) for inflections, convex and concave adaptors in Experiment 3, for three observers. Zero on the *x*-axis represents the point of veridical equality as predicted by the null hypothesis. Error bars indicate 95% confidence intervals based on 5000 bootstrap resamples. Data are also shown averaged across observers. Error bars indicate ±1 *SEM* across observers (N = 3).

(i and ii). The probe stimuli in these conditions were always whole RF patterns.

The magnitude of the aftereffect for adaptation to the whole shape, inflections, or convexities and concavities are shown in Figure 6. All observers showed a positive shift in the PSE for all adaptors (95% CIs did not include zero), indicating that an amplitude aftereffect could be generated by adaptation to the parts of the RF pattern as well as to the whole shape. The average effect sizes (±1 *SEM*, expressed as a percentage of the reference probe amplitude) were 17.13 ± 5.41% for the whole shape adaptor condition, 15.3 ± 5.37% for the inflections condition, and 16.93 ± 5.48% for the extrema condition.

Despite variation in the individual observers' data in terms of absolute magnitude, no observers showed a significant difference in the size of the effect for inflection stimuli compared to convexity and concavity stimuli (95% confidence intervals overlapped), suggesting that both extrema and inflections contributed equally to the representation of the pattern. Furthermore, the adaptive effect of the parts adaptors was not significantly different from that of the whole shape adaptor, except in one case (SH: extrema < whole shape). This might seem surprising, given the data from Experiment 1, but one must bear in mind that the presentation of the parts stimuli was different from Experiment 1. The stimuli in the present experiment used smaller sections of the contour compared to Experiment 1, but unlike Experiment 1, here we presented multiple parts of the contour in a single temporal window. This means that spatial integration (global pooling) of the parts (e.g., convex maxima) was possible by virtue of them being presented within a single temporal window. In fact, near-threshold studies of RF pattern processing have also reported that global processing of RF patterns can occur for patterns in which parts of the shape have been occluded (Bell & Badcock, 2008; Loffler et al., 2003; Poirier & Wilson, 2007). It is therefore not surprising that we obtained similar size aftereffects for parts and whole adaptors; what is of interest is the finding that curvature extrema and inflections appear to contribute equally to the overall shape representation.

Experiment 3: Comparing individual cues

Contrary to expectations from previous reports (e.g., Hess et al., 1999; Loffler et al., 2003; Poirier & Wilson, 2007), the results of Experiment 2 demonstrated no difference in the amount of adaptation generated by inflections compared to convexities and concavities, suggesting that they contribute equally to the overall shape representation. However, an alternative explanation is that convexities do contribute more than inflections, but when presented in alternation with concavities (whose

contribution had not been tested), the overall amount of adaptation is reduced. In Experiment 3, each adaptor consisted of only half the RF pattern (one of convexities, concavities, or inflections; see Figure 3Bi and ii) and we measured the change in the perceived amplitude of a whole RF pattern in the adapted visual field. This set of conditions allowed us to compare the effects of adaptation resulting from each of the part stimuli in isolation.

The magnitudes of the RFAAE for adaptors consisting of convexities only, concavities only, and inflections are shown in Figure 7. No observer showed any significant difference in adaptation between any of the three adaptor conditions (95% confidence intervals overlapped). The mean PSE shifts for inflections, convexities, and concavities (expressed as a percentage of the reference probe amplitude) were 15.5%, 16.3%, and 17.1%, respectively. This indicates that the results of Experiment 2 cannot be explained by particularly weak adaptation to the concavities; instead, all three parts of the RF pattern appear to be equally effective as adaptors. For the two observers that also took part in Experiment 2, the magnitudes of the RFAAEs were about a third lower in this experiment than in Experiment 2, reflecting the fact that the parts adaptors here contained only half of the whole contour.

General discussion

In this study, we have used the Radial Frequency (RF) pattern to investigate which parts of the pattern are used to represent its overall shape when the shape is supra-threshold. Although RF patterns have proven a popular stimulus for studying holistic shape processing (Achtman, Hess, & Wang, 2000; Almeida, Dickinson, Maybery, Badcock, & Badcock, 2010; Anderson, Habak, Wilkinson, & Wilson, 2007; Bell, Wilkinson, Wilson, Loffler, & Badcock, 2009; Jeffrey et al., 2002; Rainville & Wilson, 2005; Smith, Lee, Wolfgang, & Ratcliff, 2009) and object recognition (Poirier & Wilson, 2006, 2010; Wilkinson et al., 2007; Wilson, Loffler, & Wilkinson, 2002; Wilson & Wilkinson, 2002; Wilson et al., 2000), they have concentrated on whether global shape processes mediate the ability to discriminate an RF contour from a smooth circle. No previous studies to our knowledge have considered whether global shape processing occurs for the representation of supra-threshold RF patterns. We used the radial frequency amplitude aftereffect, or RFAAE (Bell & Kingdom, 2009) in conjunction with an established compound adaptation technique (Hancock & Peirce, 2008; Peirce & Taylor, 2006) to show that the processing of high-amplitude RF patterns also involves global shape processing (Figure 5).

Having demonstrated that a supra-threshold RF pattern is processed as a global form, we went on to show that the parts of the shape centered on points of maximum *convex* curvature, on points of maximum *concave* curvature, and on points of *inflection* contribute equally to the representation of an RF contour's shape (Figures 6 and 7). In the studies mentioned above that measured thresholds for discriminating an RF pattern from a circle, the greatest contribution was ascribed either to points of convex curvature (Habak et al., 2004; Loffler et al., 2003; Poirier & Wilson, 2007) or to the "sides" of the pattern (Hess et al., 1999; Mullen & Beaudot, 2002). However, the contribution of concave regions and of inflections cannot be determined using such a paradigm because these features are not present at low shape amplitudes. With the supra-threshold RF patterns employed here, we were able to measure the contribution of both concavities and inflections, and our results reveal that when present, both these features play a significant role in the processing of global contour shape.

Attneave (1954) was the first to suggest that concavities and convexities are important for representing objects via line drawings; however, their relative contribution was not precisely measured. More recently, convex and concave parts have been compared in terms of their relative salience (De Winter & Wagemans, 2006; Hoffman & Richards, 1984; Hoffman & Singh, 1997) and in terms of relative sensitivity to the appearance of, or change in, each type of curvature extrema (Barenholtz, Cohen, Feldman, & Singh, 2003; Bertamini, 2001, 2008; Bertamini & Farrant, 2005). A common finding among the salience studies is that concave parts are highly salient features for segmenting the parts of an object (De Winter & Wagemans, 2006; Hoffman & Singh, 1997), as proposed by Hoffman and Richards' (1984) "minima rule". As noted by De Winter and Wagemans' (2006), however, it is not clear what sort of relationship exists between the perceptual salience of a feature and its contribution to shape processing. This is an empirical question, and we make no claims about the relative saliencies of the parts stimuli used in our study. What is presented in the current study is a demonstration that adapting to either the convex or concave parts of a contour shape produces a similar shift in the overall appearance of a whole RF shape. The logical interpretation of this result is that both cues contribute equally in representing RF shapes. With regard to measures of sensitivity, studies measuring the detection of, or a change in, a curvature extrema have provided mixed reports as to whether or not we are more sensitive to one curvature extrema relative to another (e.g., Barenholtz et al., 2003; Bertamini, 2001, 2008; Bertamini & Farrant, 2005). Indeed some recent models of shape coding utilize both convexities and concavities for representing shape, without assigning greater weighting to either cue (Connor, 2004; Pasupathy & Connor, 2002). In addition, recent psychophysical evidence suggests that there are mechanisms within the brain that are selective for curves but are not selective for the sign of the curve (Bell, Gheorghiu, & Kingdom, 2009).

In addition to curvature maxima (convex and concave), we showed that inflections contribute significantly to the global representation of an RF shape. The point of inflection has been referred to in the RF literature as a zero crossing, i.e., the point where the contour passes through its mean radius. However, as noted in Figure 1 and above, a minimum amplitude in RF patterns is required before inflection points occur, so the role of inflections can only be studied with supra-threshold RF patterns. It should be noted however that ours is not the first study to show that curves containing inflections are units of information for shape processing. Gheorghiu and Kingdom (2008) showed that a half-cycle of sine-wave contour centered on the d.c. (i.e., containing an inflection at the d.c.) is an effective adaptor for a whole sine-wave test, albeit not as effective as a half-cycle centered on the peak or trough of the waveform, which has no inflection point. In addition, Pasupathy and Connor's (1999, 2001) neurophysiological studies of macaque V4 have revealed the existence of neurons that respond optimally to a contour fragment that changes in sign of curvature, i.e., that contains an inflection, rather than to one with a single sign of curvature.

A recent suggestion is that low-frequency RF patterns are processed through narrow-band contour shape channels (Bell & Badcock, 2009; Bell, Wilkinson et al., 2009; Loffler, 2008; Loffler et al., 2003). Bell, Wilkinson et al. (2009) have argued that pattern amplitude is a continuous dimension to which an RF channel is sensitive. This implies that both low- and high-amplitude RF shapes are globally processed. Many studies have shown that near-threshold (low) amplitude RF patterns are processed as global shapes (Bell & Badcock, 2008; Bell, Wilkinson et al., 2009; Hess et al., 1999; Loffler et al., 2003; Wilkinson et al., 1998), but until now there was scant evidence that this was also true for higher amplitude RF shapes. Here we have shown that a supra-threshold amplitude (high) RF pattern is processed as a global shape and that all parts of the contour contribute to global shape processing.

Acknowledgments

This research was supported by the Natural Sciences and Engineering Research Council (NSERC) of Canada (Grant OGP01217130) given to F.K. and by the Wellcome Trust, UK (Grant 085444/Z/08/Z) to J.W.P. and S.H.

Commercial relationships: none.
Corresponding author: Jason Bell.
Email: jason.bell@mail.mcgill.ca.
Address: McGill Vision Research, Department of Ophthalmology, McGill University, 687 Pine Avenue West, H4-14. Montreal, Quebec H3A 1A1, Canada.

References

Achtman, R. L., Hess, R. F., & Wang, Y. Z. (2000). Regional sensitivity for shape discrimination. *Spatial Vision, 13,* 377–391. [PubMed]

Almeida, R. A., Dickinson, J. E., Maybery, M. T., Badcock, J. C., & Badcock, D. R. (2010). A new step towards understanding Embedded Figures Test performance in the autism spectrum: The radial frequency search task. *Neuropsychologia, 48,* 374–381. [PubMed]

Anderson, N. D., Habak, C., Wilkinson, F., & Wilson, H. R. (2007). Evaluating shape after-effects with radial frequency patterns. *Vision Research, 47,* 298–308. [PubMed]

Attneave, F. (1954). Some informational aspects of visual perception. *Psychological Review, 61,* 183–193. [PubMed]

Barenholtz, E., Cohen, E. H., Feldman, J., & Singh, M. (2003). Detection of change in shape: An advantage for concavities. *Cognition, 89,* 1–9. [PubMed]

Bell, J., & Badcock, D. R. (2008). Luminance and contrast cues are integrated in global shape detection with contours. *Vision Research, 48,* 2336–2344. [PubMed]

Bell, J., & Badcock, D. R. (2009). Narrow-band radial frequency shape channels revealed by sub-threshold summation. *Vision Research, 49,* 843–850. [PubMed]

Bell, J., Badcock, D. R., Wilson, H., & Wilkinson, F. (2007). Detection of shape in radial frequency contours: Independence of local and global form information. *Vision Research, 47,* 1518–1522. [PubMed]

Bell, J., Dickinson, J. E., & Badcock, D. R. (2008). Radial frequency adaptation suggests polar-based coding of local shape cues. *Vision Research, 48,* 2293–2301. [PubMed]

Bell, J., Gheorghiu, E., & Kingdom, F. A. A. (2009). Orientation tuning of curvature adaptation reveals both curvature-polarity-selective and non-selective mechanisms. *Journal of Vision, 9*(12):3, 1–11, http://www.journalofvision.org/content/9/12/3, doi:10.1167/9.12.3. [PubMed] [Article]

Bell, J., & Kingdom, F. A. A. (2009). Global contour shapes are coded differently from their local components. *Vision Research, 49,* 1702–1710. [PubMed]

Bell, J., Wilkinson, F., Wilson, H. R., Loffler, G., & Badcock, D. R. (2009). Radial frequency adaptation reveals interacting contour shape channels. *Vision Research, 49,* 2306–2317. [PubMed]

Bertamini, M. (2001). The importance of being convex: An advantage for convexity when judging position. *Perception, 30,* 1295–1310. [PubMed]

Bertamini, M. (2008). Detection of convexity and concavity in context. *Journal of Experimental Psychology: Human Perception and Performance, 34,* 775–789. [PubMed]

Bertamini, M., & Farrant, T. (2005). Detection of change in shape and its relation to part structure. *Acta Psychology, 120,* 35–54. [PubMed]

Biederman, I. (1987). Recognition-by-components: A theory of human image understanding. *Psychological Review, 94,* 115–147. [PubMed]

Connor, C. E. (2004). Shape dimensions and object primitives. In L. M. Chalupa & J. S. Werner (Eds.), *The visual neurosciences* (pp. 1080–1089). London: MIT Press.

De Winter, J., & Wagemans, J. (2006). Segmentation of object outlines into parts: A large-scale integrative study. *Cognition, 99,* 275–325. [PubMed]

Dumoulin, S. O., & Hess, R. F. (2007). Cortical specialization for concentric shape processing. *Vision Research, 47,* 1608–1613. [PubMed]

Gallant, J. L., Braun, J., & Van Essen, D. C. (1993). Selectivity for polar, hyperbolic, and Cartesian gratings in Macaque visual cortex. *Science, 259,* 100–103. [PubMed]

Gallant, J. L., Connor, C. E., Rakshit, S., Lewis, J. W., & Van Essen, D. C. (1996). Neural responses to polar, hyperbolic, and Cartesian gratings in area V4 of the Macaque monkey. *Journal of Neurophysiology, 76,* 2718–2739. [PubMed]

Gheorghiu, E., & Kingdom, F. A. (2008). Spatial properties of curvature-encoding mechanisms revealed through the shape-frequency and shape-amplitude after-effects. *Vision Research, 48,* 1107–1124. [PubMed]

Grill-Spector, K., Kushnir, T., Edelman, S., Itzchak, Y., & Malach, R. (1998). Cue-invariant activation in object-related areas of the human occipital lobe. *Neuron, 21,* 191–202. [PubMed]

Habak, C., Wilkinson, F., Zakher, B., & Wilson, H. R. (2004). Curvature population coding for complex shapes in human vision. *Vision Research, 44,* 2815–2823. [PubMed]

Hancock, S., & Peirce, J. W. (2008). Selective mechanisms for simple contours revealed by compound adaptation. *Journal of Vision, 8*(7):11, 1–10, http://www.journalofvision.org/content/8/7/11, doi:10.1167/8.7.11. [PubMed] [Article]

Hayworth, K. J., & Biederman, I. (2006). Neural evidence for intermediate representations in object recognition. *Vision Research, 46,* 4024–4031. [PubMed]

Hess, R. F., Achtman, R. L., & Wang, Y. Z. (2001). Detection of contrast-defined shape. *Journal of the Optical Society of America A, Optics, Image Science, and Vision, 18,* 2220–2227. [PubMed]

Hess, R. F., Wang, Y. Z., & Dakin, S. C. (1999). Are judgements of circularity local or global? *Vision Research, 39,* 4354–4360. [PubMed]

Hoffman, D. D., & Richards, W. A. (1984). Parts of recognition. *Cognition, 18,* 65–96. [PubMed]

Hoffman, D. D., & Singh, M. (1997). Salience of visual parts. *Cognition, 63,* 29–78. [PubMed]

Hubel, D. H., & Wiesel, T. N. (1968). Receptive fields and functional architecture of monkey striate cortex. *The Journal of Physiology, 195,* 215–243. [PubMed]

Jeffrey, B. G., Wang, Y. Z., & Birch, E. E. (2002). Circular contour frequency in shape discrimination. *Vision Research, 42,* 2773–2779. [PubMed]

Kapadia, M. K., Westheimer, G., & Gilbert, C. D. (2000). Spatial distribution of contextual interactions in primary visual cortex and in visual perception. *Journal of Neurophysiology, 84,* 2048–2062. [PubMed]

Kourtzi, Z., & Kanwisher, N. (2001). Representation of perceived object shape by the human lateral occipital complex. *Science, 293,* 1506–1509. [PubMed]

Kurki, I., Saarinen, J., & Hyvarinen, A. (2009). Integration of contour features into a global shape: A classification image study. *Perception, 38,* ECVP Abstract Supplement, 25. [PubMed]

Ledgeway, T., & Smith, A. T. (1994). Evidence for separate motion-detecting mechanisms for first- and second-order motion in human vision. *Vision Research, 34,* 2727–2740. [PubMed]

Loffler, G. (2008). Perception of contours and shapes: Low and intermediate stage mechanisms. *Vision Research, 48,* 2106–2127. [PubMed]

Loffler, G., Wilson, H. R., & Wilkinson, F. (2003). Local and global contributions to shape discrimination. *Vision Research, 43,* 519–530. [PubMed]

Mullen, K. T., & Beaudot, W. H. (2002). Comparison of color and luminance vision on a global shape discrimination task. *Vision Research, 42,* 565–575. [PubMed]

Muller, K. M., Wilke, M., & Leopold, D. A. (2009). Visual adaptation to convexity in macaque area V4. *Neuroscience, 161,* 655–662. [PubMed]

Pasupathy, A., & Connor, C. E. (1999). Responses to contour features in macaque area V4. *Journal of Neurophysiology, 82,* 2490–2502. [PubMed]

Pasupathy, A., & Connor, C. E. (2001). Shape representation in area V4: Position-specific tuning for boundary conformation. *Journal of Neurophysiology, 86,* 2505–2519. [PubMed]

Pasupathy, A., & Connor, C. E. (2002). Population coding of shape in area V4. *Nature Neuroscience, 5,* 1332–1338. [PubMed]

Peirce, J. W. (2007). PsychoPy—Psychophysics software in Python. *Journal of Neuroscience Methods, 162,* 8–13. [PubMed]

Peirce, J. W., & Taylor, L. J. (2006). Selective mechanisms for complex visual patterns revealed by adaptation. *Neuroscience, 141,* 15–18. [PubMed]

Poirier, F. J., & Wilson, H. R. (2007). Object perception and masking: Contributions of sides and convexities. *Vision Research, 47,* 3001–3011. [PubMed]

Poirier, F. J. A. M., & Wilson, H. R. (2006). A biologically plausible model of human radial frequency perception. *Vision Research, 46,* 2443–2455. [PubMed]

Poirier, F. J. A. M., & Wilson, H. R. (2010). A biologically plausible model of human shape symmetry perception. *Journal of Vision, 10*(1):9, 1–16, http://www.journalofvision.org/content/10/1/9, doi:10.1167/10.1.9. [PubMed] [Article]

Rainville, S. J., & Wilson, H. R. (2005). Global shape coding for motion-defined radial-frequency contours. *Vision Research, 45,* 3189–3201. [PubMed]

Smith, P. L., Lee, Y. E., Wolfgang, B. J., & Ratcliff, R. (2009). Attention and the detection of masked radial frequency patterns: Data and model. *Vision Research, 49,* 1363–1377. [PubMed]

Wilkinson, F., James, T. W., Wilson, H. R., Gati, J. S., Menon, R. S., & Goodale, M. A. (2000). An fMRI study of the selective activation of human extrastriate form vision areas by radial and concentric gratings. *Current Biology, 10,* 1455–1458. [PubMed]

Wilkinson, F., Shahjahan, S., & Wilson, H. (2007). Hysteresis between shape-defined categories [Abstract]. *Journal of Vision, 7*(9):209, 209a, http://www.journalofvision.org/content/7/9/209, doi:10.1167/7.9.209.

Wilkinson, F., Wilson, H. R., & Habak, C. (1998). Detection and recognition of radial frequency patterns. 3555–3568. [PubMed]

Wilson, H. R., Loffler, G., & Wilkinson, F. (2002). Synthetic faces, face cubes, and the geometry of face space. *Vision Research, 42,* 2909–2923. [PubMed]

Wilson, H. R., & Wilkinson, F. (2002). Symmetry perception: A novel approach for biological shapes. *Vision Research, 42,* 589–597. [PubMed]

Wilson, H. R., Wilkinson, F., Lin, L. M., & Castillo, M. (2000). Perception of head orientation. *Vision Research, 40,* 459–472. [PubMed]